

The Plastidic Bile Acid Transporter 5 Is Required for the Biosynthesis of Methionine-Derived Glucosinolates in *Arabidopsis thaliana* ^W

Tamara Gigolashvili,^a Ruslan Yatusevich,^a Inga Rollwitz,^a Melanie Humphry,^a Jonathan Gershenzon,^b and Ulf-Ingo Flügge^{a,1}

^aBotanisches Institut der Universität zu Köln, D-50931 Köln, Germany

^bMax-Planck-Institut für Chemische Ökologie, D-07745 Jena, Germany

Aliphatic glucosinolate biosynthesis is highly compartmentalized, requiring import of 2-keto acids or amino acids into chloroplasts for side chain elongation and export of the resulting compounds into the cytosol for conversion into glucosinolate. Aliphatic glucosinolate biosynthesis in *Arabidopsis thaliana* is regulated by three R2R3-MYB transcription factors, the major player being High Aliphatic Glucosinolate 1 (HAG1/MYB28). Here, we show that *BAT5*, which belongs to the putative bile acid transporter family, is the only member of this family that is transactivated by HAG1/MYB28, HAG2/MYB76, and HAG3/MYB29. Furthermore, two isopropylmalate isomerases genes, *IPMI1* and *IPMI2*, and the isopropylmalate dehydrogenase gene, *IPMDH1*, were identified as targets of HAG1/MYB28 and the corresponding proteins localized to plastids, suggesting a role in plastidic chain elongation reactions. The *BAT* proteins also localized to plastids; however, only mutants defective in *BAT5* function contained strongly reduced levels of aliphatic glucosinolates. The *bat5* mutant chemotype was rescued by induced overexpression of *BAT5*. Feeding experiments using 2-keto acids and amino acids of different chain length suggest that *BAT5* is a plastidic transporter of (chain-elongated) 2-keto acids. Mechanical stimuli and methyl jasmonate transiently induced *BAT5* expression in inflorescences and leaves. Thus, *BAT5* was identified as the first transporter component of the aliphatic glucosinolate biosynthetic pathway.

INTRODUCTION

Aliphatic glucosinolates mainly present in the *Brassicaceae* family, including the model plant *Arabidopsis thaliana*, comprise primarily Met-derived secondary metabolites (Kliebenstein et al., 2001; Mithen, 2001). These compounds and their breakdown products, for example, isothiocyanates, protect plants against herbivores and pathogens (Giamoustaris and Mithen, 1995; Mari et al., 1996; Manici et al., 2000; Reymond et al., 2004; Chung et al., 2005; Mewis et al., 2005; Brader et al., 2006) and are known to serve as human anticancer agents (Talalay and Fahey, 2001; Traw et al., 2003; Hayes et al., 2008). After Met-derived glucosinoates, indolic and benzyl glucosinolates are the most abundant glucosinolates in *Arabidopsis*. Although the metabolism of aliphatic glucosinolate has been extensively studied in *Arabidopsis*, not all genes in the biosynthetic pathway have been characterized yet.

The biosynthesis of Met-derived glucosinolates starts in the cytosol, where Met is transaminated by a recently characterized aminotransferase, BCAT4 (Schuster et al., 2006). The resulting 2-keto acid, 4-methylthio-2-oxobutanoate (MTOB), is thought to be imported into the chloroplast by a yet unidentified transporter,

where it reacts with acetyl-CoA in a condensation reaction catalyzed by the methylthiomalate synthases MAM1 to MAM3 to form 2-(2'-methylthio) ethylmalate, a 2-alkylmalic acid (Kroymann et al., 2001; Textor et al., 2004; Textor et al., 2007). The 2-alkylmalic acid is converted to 3-(2'-methylthio) ethylmalate, a 3-alkylmalic acid by a still unidentified isomerase, most probably an isopropylmalate isomerase (IPMI; Schuster et al., 2006). The 3-alkylmalic acid undergoes oxidative decarboxylation to yield 5-methylthio-2-oxopentanoate (MTOB), a 2-keto acid with one additional carbon in the side chain. This reaction is assumed to be catalyzed by a yet unidentified isopropylmalate dehydrogenase (IPMDH). The resulting 2-keto acid can then enter a new condensation cycle, thus creating homoketo acids of increasing side chain length (Grubb and Abel, 2006; Halkier and Gershenzon, 2006). The homoketo acids could be subsequently transaminated to corresponding chain-elongated amino acids, in the case of Met, resulting in homomethionine. These reactions are assumed to be catalyzed by the chloroplastic BCAT3 or the cytosolic BCAT4, which have been recently shown to transaminate short-chained homoketo acids generated in the glucosinolate biosynthetic pathway (Knill et al., 2008). It is therefore expected that either the Met-derived chain-elongated 2-keto acid (if the second transamination step is performed in the cytosol by BCAT4 or a yet unknown BCAT) or the chain-elongated amino acid (if the second transamination is performed by the plastidic BCAT3) must be exported from the chloroplast into the cytosol by so far unknown transporter(s) to be further converted into glucosinolates.

¹ Address correspondence to ui.fluegge@uni-koeln.de.

The author responsible for distribution of materials integral to the findings presented in this article in accordance with policy described in the Instruction of Authors (www.plantcell.org) is: Ulf-Ingo Flügge (ui.fluegge@uni-koeln.de).

^WOnline version contains Web-only data.

www.plantcell.org/cgi/doi/10.1105/tpc.109.066399

The following cytosolic steps involve oxidation of the chain-elongated amino acid to an aldoximine catalyzed by the cytochrome P450 monooxygenases CYP79F1 and CYP79F2 (Hansen et al., 2001; Reintanz et al., 2001; Chen et al., 2003; Tantikanjana et al., 2004). A second oxidation step leads to an *aci*-nitro compound, catalyzed by CYP83A1 (Hemm et al., 2003; Naur et al., 2003), which is then conjugated with a sulfur donor into *S*-alkyl thiohydroximate. The final biosynthetic steps comprise consecutive actions catalyzed by C-S lyases (Mikkelsen et al., 2004), UDP-glucosyltransferases (Grubb et al., 2004), and sulfotransferases (ST5b and ST5c; Piotrowski et al., 2004). Recently, the R2R3-MYB transcription factors HAG1/MYB28, HAG2/MYB76, and HAG3/MYB29 were identified as regulators of Met-derived glucosinolate biosynthesis, with High Aliphatic Glucosinolate 1 (HAG1/MYB28) being the main player (Gigolashvili et al., 2007, 2008; Hirai et al., 2007; Sønderby et al., 2007). Here, we describe the identification of novel target genes of the HAG1/MYB28 transcription factor and provide evidence that BAT5 annotated as a bile acid transporter is involved in the transport of 2-keto acids between chloroplasts and the cytosol.

RESULTS

Identification of Novel HAG1/MYB28 Target Genes Involved in the Met Chain Elongation Pathway

As demonstrated recently, the R2R3-MYB transcription factor HAG1/MYB28 is the key player in the regulation of aliphatic glucosinolate biosynthesis (Gigolashvili et al., 2007; Hirai et al., 2007). To identify novel target genes of HAG1/MYB28, we

analyzed publicly available transcriptome gene coexpression profiles for putative interacting factors (Table 1). Coexpressed genes include known genes of the aliphatic glucosinolate biosynthetic pathway, such as *BCAT4*, *MAM1*, *CYP83A1*, *CYP79F1*, *BCAT3*, the sulfotransferases *ST5b/c*, and the C-S lyase, but also putatively involved genes, such as the IPMIs *IPMI1* and *IPMI2*, the isopropylmalate dehydrogenase *IPMDH1*, and a gene encoding a putative transporter, *BAT5*, which has been annotated as a bile acid transporter and belongs to a small gene family comprising five members (*BAT1* to *BAT5*). Several genes identified by this approach were subjected to a real-time PCR analysis using mRNA of wild-type and *HAG1/MYB28* overexpression plants to verify putative target genes.

As shown in Figure 1A, the steady state transcript levels of several novel putative glucosinolate biosynthetic genes were significantly increased in the *HAG1/MYB28* overexpression lines compared with the wild type. This holds true for the two IPMIs, *IPMI1* and *IPMI2*, the isopropylmalate dehydrogenase *IPMDH1*, the recently characterized branched-chain aminotransferase *BCAT3*, and *BAT5*. The expression of other members of the bile acid transporter family (i.e., *BAT1*, -2, -3, and -4) and of *BCAT5* as well as *IPMI3*, *IPMDH2*, and *IPMDH3* remained almost unaffected.

Furthermore, the ability of HAG1/MYB28 to activate promoters of the identified candidate genes was analyzed in cotransformation assays (Berger et al., 2007). Cultured *Arabidopsis* Columbia-0 (Col-0) cells were infiltrated with a supervirulent *Agrobacterium tumefaciens* strain carrying the *HAG1/MYB28* construct for effector expression and different reporter constructs containing the *uidA* (β -glucuronidase [*GUS*]) gene driven by the promoters of the candidate genes. As shown in Figure 1B, *Arabidopsis* cells

Table 1. Putative Target Genes of HAG1/MYB28 with Defined or Suggested Functions in GS Metabolism Identified by Gene Coexpression Analysis Using a Publicly Available Microarray Data Set (<http://atted.jp/>)

AGI	NAME	References	COR ^a
At5g61420	Transcription factor HAG1/MYB28	Hirai et al. (2007) Gigolashvili et al. (2007) Sønderby et al. (2007)	
At4g13770	CYP83A1	Hemm et al. (2003) Naur et al. (2003)	0.80
At3g58990	IPMI1	Actual work	0.78
At4g12030	Putative bile acid transporter (BAT5)	Actual work	0.77
At1g74090	St5b	Piotrowski et al. (2004)	0.76
At5g23010	MAM1	Kroymann et al. (2001)	0.70
At2g43100	IPMI2	Actual work	0.74
At2g31790	UDP glucosyltransferase	Grub and Abel. (2006)	0.72
At3g19710	BCAT4	Schuster et al. (2006)	0.68
At1g16410	CYP79F1	Reintanz et al. (2001)	0.67
At1g62650	Flavin-containing monooxygenase	Hansen et al. (2001) Chen et al. (2003) Li et al. (2008)	0.67
At1g31180	IPMDH	Actual work	0.66
At1g18590	St5c	Piotrowski et al. (2004)	0.61
At1g65860	Flavin-containing monooxygenase FMO3	Li et al. (2008)	0.54
At2g20610	C-S lyase	Mikkelsen et al. (2004)	0.53
At3g49680	BCAT3	Knill et al. (2008)	0.53
At4g39940	Adenosine-5-phosphosulfate-kinase	Mugford et al. (2009)	0.49

^aPearson's correlation coefficient.

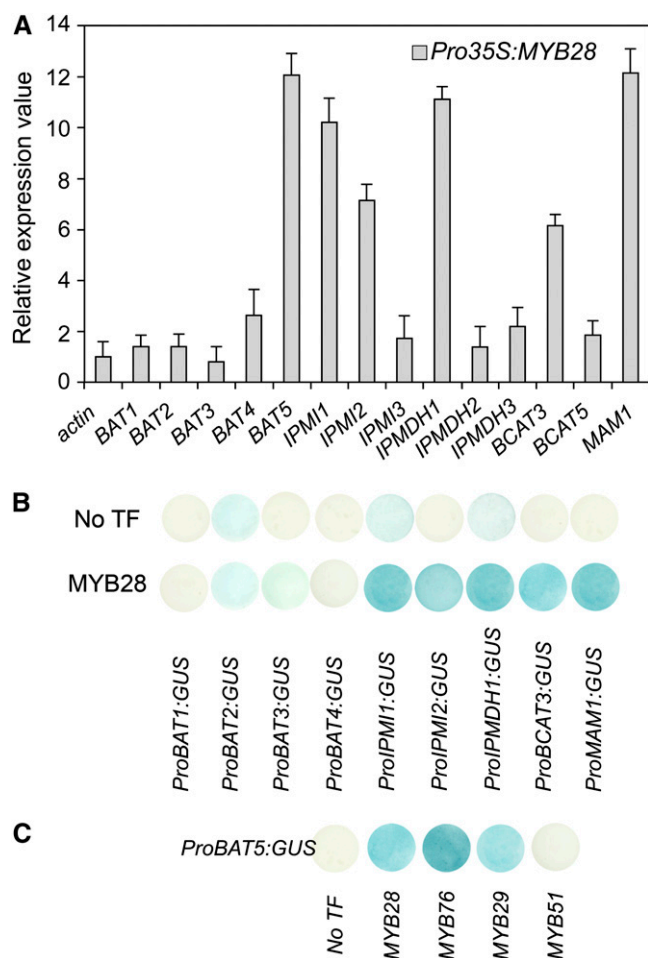


Figure 1. Identification of Novel Genes Involved in Met-Derived Glucosinolate Biosynthesis Using Real-Time PCR Analysis and Cotransformation Assays in Cultured *Arabidopsis* Cells.

(A) Transcript levels of predicted glucosinolate pathway genes in rosette leaves of 5-week-old HAG1/MYB28 overexpression plants. Relative gene expression values are given compared with the wild type (=1). Means \pm SD ($n = 3$).

(B) Cotransformation assays for the determination of target gene specificity of HAG1/MYB28 (effector) toward target promoters of predicted aliphatic biosynthetic pathway genes are shown. The promoters of *BAT1*, *BAT2*, *BAT3*, *BAT4*, *IPMI1*, *IPMI2*, *IPMDH1*, and *BCAT3* genes were fused to the *uidA* (*GUS*) reporter gene (*TargetPromoter:GUS* vectors). The promoter of the *MAM1* gene was used as a positive control. Cultured *Arabidopsis* cells were inoculated with the supervirulent *Agrobacterium* strain LBA4404.pBRR1MCS.virGN54D containing either only the reporter construct (*TargetPromoter:GUS:pGWB3i*) or the reporter construct and the HAG1/MYB28 effector construct (*Pro35S:HAG1:pGWB2*). GUS staining indicates transactivation of a given promoter by an effector.

(C) Transactivation of *ProBAT5:GUS* by HAG1/MYB28, HAG2/MYB76, HAG3/MYB29, and HIG1/MYB51.

transiently expressing both reporter and effector constructs showed significantly increased GUS activities for *IPMI1*, *IPMI2*, *IPMDH1*, *BCAT3*, and *BAT5*, demonstrating the potential of HAG1/MYB28 to transactivate respective promoters of biosynthetic genes as well as that of the putative bile acid transporter

BAT5. Finally, it is also evident from Figure 1C that the transactivation capacity of the other two regulators of aliphatic glucosinolate biosynthesis, HAG2/MYB76 and HAG3/MYB29, toward the *BAT5* promoter is comparable with that of the main regulator HAG1/MYB28.

BAT5 Is Ubiquitously Expressed and Is Localized to Plastids, as Are IPMI1, IPMI2, and IPMDH1

Due to significant sequence similarities to mammalian sodium-coupled bile acid transporters (Hagenbuch et al., 1991; Wong et al., 1994; Trauner and Boyer, 2003), the five BAT proteins were assigned as *Arabidopsis* bile acid transporters, although their actual function is unknown. All five members of the BAT family in *Arabidopsis* have eight to nine predicted transmembrane spans (<http://aramemnon.botanik.uni-koeln.de/index.ep>; Schwacke et al., 2003), indicating that all BAT members presumably function as membrane-integrated transporter proteins. BLAST searches using the *Arabidopsis* BAT protein sequences revealed that *Oryza sativa* also possesses five different BAT proteins (Rzewuski and Sauter, 2002) and that a large number of ESTs encoding plant BAT proteins can be found throughout the plant kingdom and in a variety of bacteria (Figure 2; see Supplemental Data Set 1 online). Whereas the only bacterial putative BAT ortholog was recently identified as a cholate transporter named Ctr in *Bifidobacterium longum* (Price et al., 2006), the function(s) of the plant proteins remains to be elucidated.

For a detailed analysis of the organ- and tissue-specific expression profile of the *BAT5* gene, a translational fusion of the *BAT5* promoter containing the first exon with the *uidA* (*GUS*) gene was analyzed for GUS activity in several transgenic *Arabidopsis* lines. As shown in Figure 3, *BAT5* is strongly expressed in all organs in young seedlings and in leaves and roots of mature plants. High GUS activity could also be detected in sepals, stamens, and in pollen grains. The GUS expression profiles of the other *Arabidopsis* BAT genes are given as supplementary material, showing overlapping but distinct expression patterns (see Supplemental Figure 1 online).

In contrast with the mammalian proteins, the *Arabidopsis* BATs possess N-terminal extensions of ~60- to 80-amino acid residues in length that might function to target the proteins to specific cellular compartments. All *Arabidopsis* BAT proteins were indeed predicted to be localized to plastids and, in some cases, also to mitochondria (<http://aramemnon.botanik.uni-koeln.de/index.ep>; Schwacke et al., 2003). To assess the subcellular localization of *BAT5* along with that of *IPMI1*, *IPMI2*, and *IPMDH1*, which have also been identified as novel target genes of HAG1/MYB28 (Figure 1), the full-length coding sequence of the *BAT5* gene (1221 bp) and the N-terminal sequences, including the putative plastidic targeting peptides (as predicted by TargetP) of *BAT5* (252 bp), *IPMI1* (321 bp), *IPMI2* (303 bp), and *IPMDH1* (288 bp), were translationally fused to green fluorescent protein (*GFP*). These constructs were introduced into cultured *Arabidopsis* cells and/or adult leaves of *Arabidopsis* wild-type plants by infiltration with *A. tumefaciens*. As demonstrated in Figure 4, GFP fused to N-terminal fragments of *BAT5*, *IPMI1*, *IPMI2*, and *IPMDH1*, as well as the plastidic triose phosphate/phosphate translocator, which was used as a positive control, all localized to plastids of

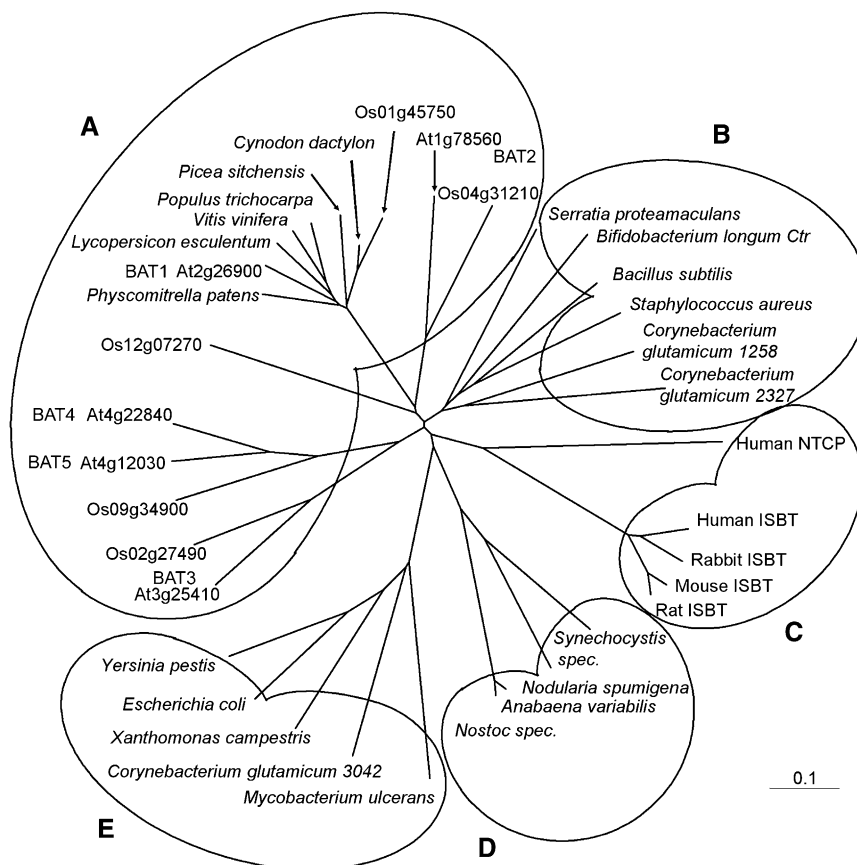


Figure 2. Phylogenetic Relationship Analysis of Bile Acid Transporter(-Like) Proteins.

The corresponding amino acid sequences were aligned with the ClustalX program, and an unrooted tree was calculated using TreeView software. Species and gene names are indicated. Cluster A, plants; B, heterotrophic bacteria group I; C, mammalia; D, cyanobacteria; E, heterotrophic bacteria group II. Ctr, chololate transporter; NTCP, Na^+ /taurochololate cotransporting peptide; ISBT, ileal sodium-dependent bile acid transporter.

cultured *Arabidopsis* cells (Figures 4A to 4F). Likewise, the full-length BAT5-GFP construct localized to chloroplasts when transiently expressed in *Arabidopsis* leaves (Figures 4G to 4I). Both the GFP fluorescence signal of BAT5-GFP (Figure 4G) and the chlorophyll autofluorescence signal (Figure 4H) colocalized to the same compartments representing chloroplasts (Figure 4I). Notably, the other members of the *Arabidopsis* BAT family were also shown to be plastid-localized (see Supplemental Figure 2 online).

The *bat5* Knockdown Mutant, Cultured *Pro35S::amiBAT5 Arabidopsis* Cells, and Stably Transformed *Pro35S::amiBAT5* Plants Contain Reduced Levels of Aliphatic Glucosinolates

To assess the function of BAT5 in the biosynthesis of aliphatic glucosinolates, two publicly available knockout lines for BAT5, SALK_126525 and SALK_126515, were analyzed at the genomic level. The SALK_126515 line turned out not to contain any T-DNA insertion. On the other hand, a T-DNA insertion in the *BAT5* gene within the SALK_126525 line could be confirmed, and a homozygous loss-of-function allele of the *BAT5* gene (*bat5*) could be isolated. Analysis of the *bat5* mutant genomic DNA by PCR with

gene-specific and T-DNA border-specific primers indicated that the T-DNA insertion was not in the first intron as annotated by SALK, but 180 bp upstream of the start codon of the *BAT5* gene (At4g12030.2). However, even this insertion led to drastically reduced steady state levels of *BAT5* mRNA in different mutant plants of the same line (*bat5-a*, *-b*, and *-c*), as revealed by real-time PCR analysis (Figure 5A). The *bat5* mutant lines showed no visible effects on plant growth and morphology under the given growth conditions.

For metabolite analysis, glucosinolates (GSs) were extracted from freeze-dried rosette leaves of 5-week-old *bat5* plants, and the levels of 3-methylsulfinylpropyl-GS (3MSOP), 4-methylsulfinylbutyl-GS (4MSOB), 5-methylsulfinylpentyl-GS (5MSOP), 7-methylsulfinylheptyl-GS (7MSOH), 8-methylsulfinyloctyl-GS (8MSOO), indol-3-ylmethyl-GS (I3M), 4-methoxyindol-3-ylmethyl-GS (4MOI3M), and 1-methoxyindol-3-ylmethyl-GS (1MOI3M) were determined. As shown in Figure 5D, *bat5* contained significantly reduced levels of the aliphatic GSs 3MSOB, 4MSOB, 7MSOH, and 8MSOO compared with the wild type. The content of total Met-derived GSs was reduced from 16 nmol/mg dry weight in the wild type to 8 nmol/mg dry weight in the *bat5* mutant, corresponding to a 50% reduction, mainly due to the



Figure 3. Histochemical GUS Staining in Tissues of *ProBAT5:GUS* Plants.

- (A) A 14-day-old seedling.
 (B) Adult leaf with cut site at the petiole.
 (C) Flower.
 (D) Silique.
 (E) Roots of adult plants.
 (F) GUS induction at cut site of inflorescence.

Bars = 500 μm in (A) and (F), 1000 μm in (B), and 150 μm in (C) to (E).

reduced content of the most abundant Met-derived GS 4MSOB. 4MSOB was reduced from 12 nmol/mg dry weight in the wild type to 6 nmol/mg dry weight in *bat5* (Figure 5D). By contrast, the content of indolic GSs, I3M, 4MOI3M, and 1MOI3M, was slightly increased in the *bat5* mutant, most likely as a result of the negative feedback regulation of Trp- and Met-derived GS biosynthetic pathways (Grubb and Abel, 2006; Givolashvili et al., 2008).

As no other *BAT5* loss-of-function mutant was available for analysis, artificial *BAT5* microRNA-overexpressing lines were established (Schwab et al., 2006). Synthetic microRNA for the *BAT5* gene (*amiBAT5* 5'-GCGGUCCUCGUUACACCU-AUG-3') was designed at <http://wmd.weigelworld.org/cgi-bin/mirnatools.pl> using the WMD version 1 software, and a transgenic *Arabidopsis* cell culture and stably transformed *Arabidopsis* plants were generated. In each case, the residual *BAT5* transcript levels (Figures 5B and 5C) and the GS content (Figures 5E and 5F) were measured in three representative lines. As shown in Figure 5B, the *BAT5* transcripts were below the detection limit in cultured cells (lines *Pro35S:amiBAT5*-1, -2, and -3) 5 to 7 d after transfection, and the content of the main aliphatic GS, 4MSOB, could not be detected at all in these lines. The stably transformed transgenic lines carrying the *Pro35S:amiBAT5* construct (*Pro35S:amiBAT5*-1, -7, and -14) showed a 60 to 80% decreased steady state level of the *BAT5* mRNA (Figure 5C), and the short-chain and long-chain aliphatic GS contents were 35 to 40% those of wild-type levels (Figure 5F). Remarkably, both the

Pro35S:amiBAT5 cell lines and the stably transformed artificial micro RNA (*ami*) plants contained slightly decreased levels of indolic GSs, which was opposite to the *bat5* mutant that showed a slight upregulation of indolic GSs (Figure 5D).

The downregulation of indolic GSs in *Pro35S:amiBAT5* lines does not seem to be related to the loss of the *BAT5* gene, but to side effects of the *amiRNA* construct that inhibit the biosynthesis of indolic GSs. This suggestion is supported by the observation that stably transformed *Pro35S:amiBAT5* lines but not the *bat5* mutant contained decreased steady state transcript levels of *MYB34*, one of the regulators of indolic GS biosynthesis (see Supplemental Figure 3 online). Changes in the transcript levels of other regulators of indolic (i.e., High Indolic Glucosinolate 1 [HIG1/MYB51] and HIG2/MYB122) and aliphatic GS biosynthesis (i.e., HAG1/MYB28, HAG3/MYB29, and HAG2/MYB76) were comparable in both *Pro35S:amiBAT5* lines and the *bat5* mutant (see Supplemental Figure 3 online). The obtained data are in accordance with the recent finding that *MYB34* plays a special role in balancing metabolic networks between aliphatic and indolic GSs (Malitsky et al., 2008). Taken together, both the analysis of the *bat5* knockdown mutant and of *Pro35S:amiBAT5* lines showed reduced levels of Met-derived GSs compared with the wild type, indicating a role for *BAT5* in the transport of chain-elongated Met derivatives between the plastids and the cytosol.

Double *bat5 bat4* and Triple *bat5 bat4 bat3* Mutants Contain GS Levels Comparable to Those of the *bat5* Mutant

Although the overexpression of *HAG1/MYB28* lead neither to an increase in the steady state mRNA levels of other *BAT* genes (Figure 1A) nor to the transactivation of these genes (Figure 1B), some functional redundancy within the *BAT* family cannot be excluded. To analyze whether or not the closest homologs of *BAT5* (i.e., *BAT4* and *BAT3*; Figure 2), are involved in the biosynthesis of GSs, homozygous knockout lines for *BAT4* (SALK_044369) and *BAT3* (Gabi-Kat479D02) were isolated, and double *bat5 bat4* and triple *bat5 bat4 bat3* homozygous knockout mutants were generated (Figures 6A and 6B). Homozygous double and triple knockout lines were confirmed by PCR using genomic DNA of mutants, and the loss of transcripts was confirmed by the analysis of mRNA levels of the corresponding genes by RT-PCR (Figure 6B). Single *bat4* and *bat3* T-DNA insertion lines as well as double *bat5 bat4* and triple *bat5 bat4 bat3* mutants did not show any phenotypic differences compared with Col-0. As shown in Figure 6C, *bat4* and *bat3* single mutants contained wild-type levels of GSs, whereas *bat5 bat4* and *bat5 bat4 bat3* showed GS profiles resembling those of the *bat5* single mutant. Together, these results demonstrate that *BAT5* is the only member of the *BAT* family that is activated by MYB transcription factors and is involved in the biosynthesis of aliphatic GSs.

Induced Expression of *BAT5* Leads to an Increased Production of Aliphatic GSs and Complementation of the *bat5* Mutant Chemotype

To restore *BAT5* activity in the *bat5* mutant, a gene complementation experiment was performed. Because constitutive

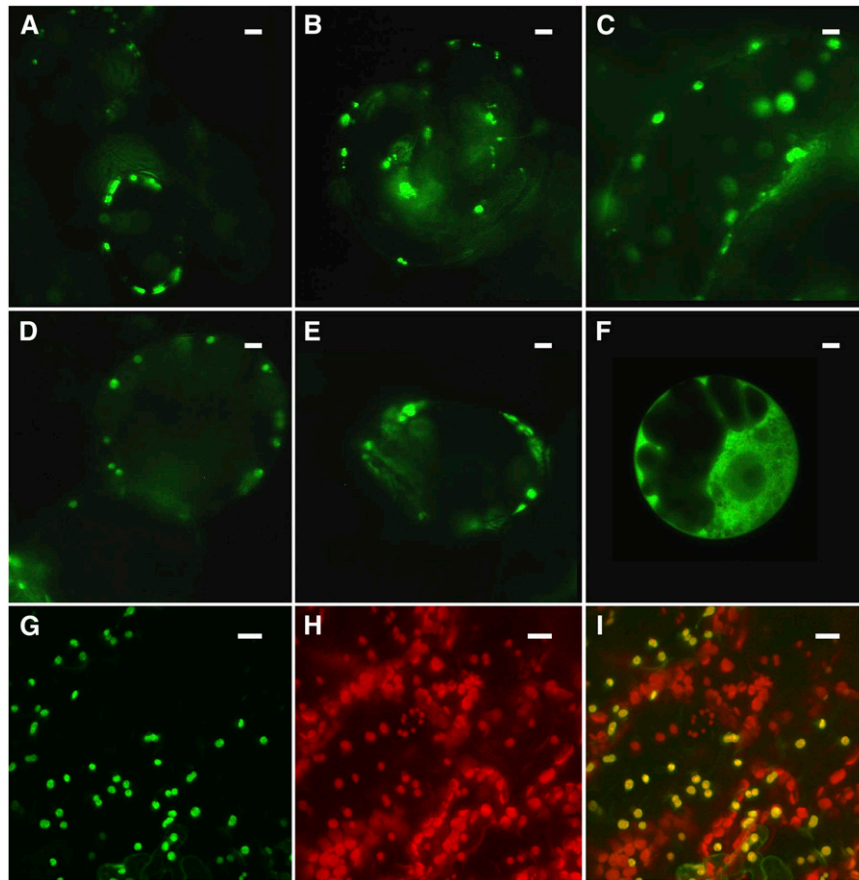


Figure 4. BAT5, IPMI1, IPMI2, and IPMDH1 Localize to Plastids.

Plastidic localization of GFP fused to N-terminal fragments of BAT5, IPMI1, IPMI2, and IPMDH1 in cultured *Arabidopsis* cells [(A) to (F)] and localization of the BAT5 full-length-GFP construct to chloroplasts of *Arabidopsis* leaves [(G) to (I)]. The patterns of fluorescence were analyzed by fluorescence [(A) to (F)] or confocal [(G) to (I)] microscopy.

(A) IPMI1.

(B) IPMI2.

(C) IPMDH1.

(D) BAT5.

(E) Triose phosphate/phosphate translocator (positive control for plastidic localization).

(F) Empty vector pGWB2-GFP (cytosolic localization of GFP).

(G) BAT5-GFP localization to chloroplasts of *Arabidopsis* leaves.

(H) Autofluorescence of chloroplasts (red).

(I) Overlay for BAT5-GFP and chloroplast autofluorescence (yellow). Bar = 10 μm . For details, see text and Methods.

overexpression of genes often leads to pleiotropic effects, *BAT5* expression in the *bat5* background was controlled by the estrogen receptor-based inducible system. The binary gateway vector used for plant transformation harbored the *BAT5-uidA* gene within recombination attR sites driven by the XVE-inducible expression system and the constitutive G10-90 promoter. This estradiol-inducible vector is identical to pER8 (Zuo et al., 2000), except that the multiple cloning site also contains recombination sites for Gateway cloning. The chemical induction followed by GUS staining of transformed plants thus allowed us to estimate the efficiency of *BAT5* induction. After treating plants with β -estradiol, leaves of 35 independent transgenic lines were tested for GUS activity, and 15 lines showing moderate to high *uidA* expression levels were

selected for chemotype analysis. The results for several representative lines (complemented *bat5/BAT5* lines) are shown in Figure 7.

Generally, the level of GUS expression (Figure 7A) correlated well with the levels of aliphatic GSs (Figure 7B) in complemented *bat5* lines. The content of total GSs increased from 50% in the *bat5* mutant to almost wild-type levels in complemented *bat5/BAT5* lines with moderate or high GUS expression levels. As evident from Figure 7B, the majority of the complemented lines contained increased levels of both short- and long-chain Met-derived GSs, including of the most abundant 4MSOB. Remarkably, the slightly increased levels of indolic GSs in the *bat5* mutant were also restored to wild-type levels in the complemented *bat5/BAT5* lines (Figure 7C).

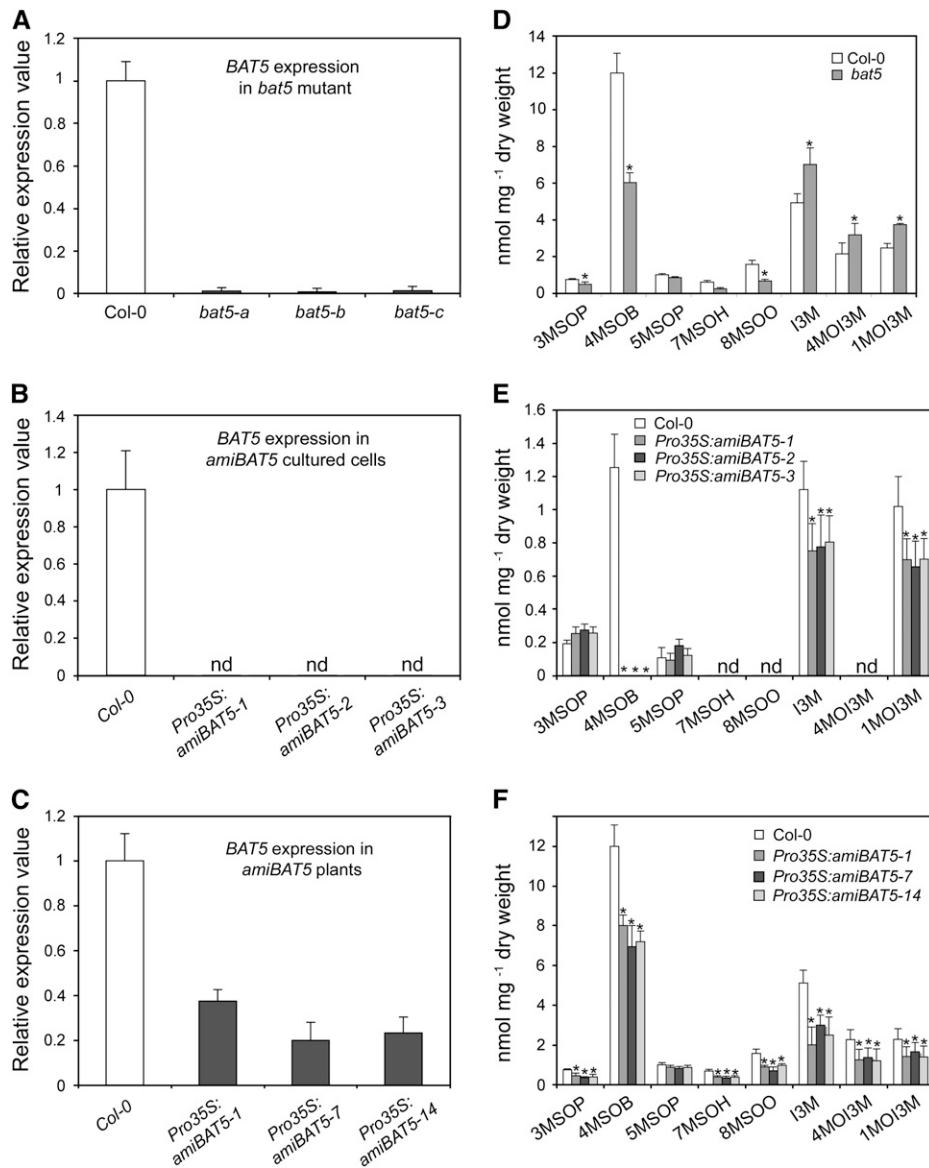


Figure 5. Analyses of the *bat5* Mutant, Cultured *Pro35S:amiBAT5 Arabidopsis* Cells, and Stably Transformed *Pro35S:amiBAT5* Plants.

(A) to (C) Steady state level of *BAT5* mRNA in three different plants of the *bat5* mutant (A), cultured *Pro35S:amiBAT5 Arabidopsis* cells (B), and stably transformed *Pro35S:amiBAT5* plants (C). Relative gene expression values are given in comparison with the wild-type (Col-0) plants or wild-type cells (wild type = 1). Means ± SD (n = 3). nd, not detectable.

(D) Contents of GSs (nmol/mg dry weight) in *bat5* mutant plants in comparison with the wild type (Col-0). Means ± SD (n = 5).

(E) Contents of GSs (nmol/mg dry weight) in *Pro35S:amiBAT5* cultured *Arabidopsis* cell lines in comparison with wild-type cells. The levels of long-chained aliphatic GSs were below the detection limit in both wild-type cells extracts and in *Pro35S:amiBAT5* cells. Means ± SD (n = 3).

(F) Contents of GSs (nmol/mg dry weight) in *Pro35S:amiBAT5* stably transformed *Arabidopsis* plants in comparison with cultured wild-type cells. Means ± SD (n = 5). Asterisk indicates significant difference in comparison to the wild-type Col-0 (Student's *t* test, P < 0.05).

Transcription of *BAT5* Is Triggered by Wounding and Induced by Methyl Jasmonate

Transcription of GS biosynthetic genes and of the regulators of GS biosynthesis has been shown to be induced by wounding (Schuster et al., 2006; Gigolashvili et al., 2007a, 2007b, 2008). To analyze whether *BAT5* promoter activity is indeed induced by

wounding, leaves and inflorescences of *ProBAT5:GUS* plants were examined at cut sites for GUS activity. As shown in Figures 3B and 3F, GUS staining was increased at the cut surface of the petiole and inflorescence close to the wounding sites.

To get more information about the time dependence of the *BAT5* response, a real-time RT-PCR analysis of wounded

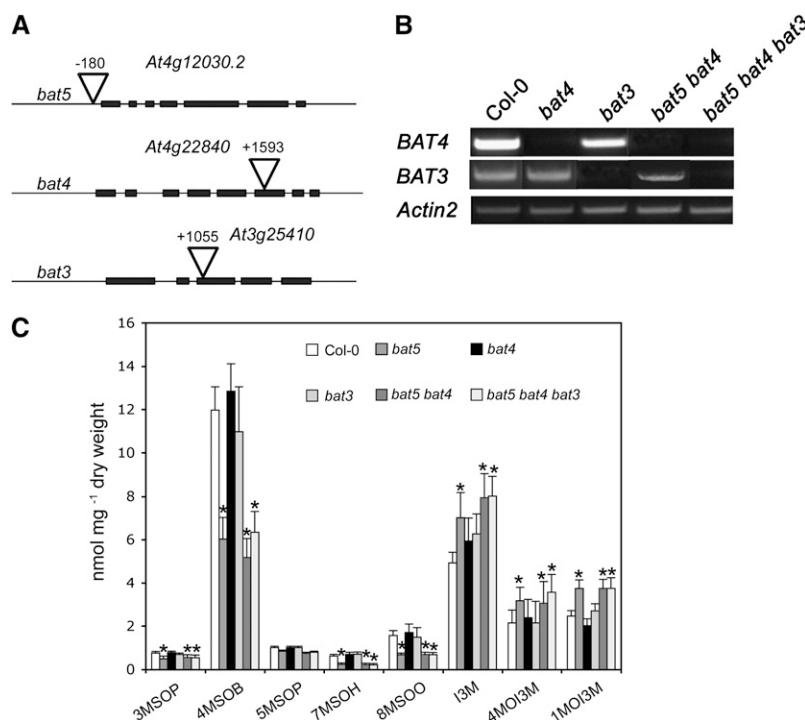


Figure 6. BAT4 and BAT3 Are Not Involved in Aliphatic GS Biosynthesis.

(A) Positions of T-DNA insertions in *BAT5*, *BAT4*, and *BAT3* genes.

(B) Confirmation of the knockout status of plants homozygous for the T-DNA insertion by RT-PCR. The cDNAs from mutant plants were amplified using primers specific to the coding regions of the corresponding *BAT* genes. The *ACTIN2* gene was used as an endogenous control.

(C) Contents of GSs (nmol/mg dry weight) in *bat4*, *bat3*, *bat5 bat4*, and *bat5 bat4 bat3* mutant plants in comparison with *bat5* and wild-type plants (Col-0). Means \pm SD ($n = 5$). Asterisk indicates significant difference in comparison to the wild-type Col-0 (Student's *t* test, $P < 0.05$).

wild-type inflorescences was performed. Figure 8A shows that the *BAT5* expression level increased by ~ 10 -fold within 5 min of wounding and started to drop to the initial level after 10 min.

Since GS biosynthesis is known to be induced by methyl jasmonate (MeJa) and salicylic acid (SA) treatment (Brader et al., 2001; Mikkelsen and Halkier, 2003; Cipollini et al., 2004; Devoto and Turner, 2005; Mewis et al., 2005; Sasaki-Sekimoto et al., 2005), and as HAG3/MYB29, an important regulator of Met-derived GS biosynthesis, is induced by MeJa (Gigolashvili et al., 2008), we asked whether or not *BAT5* is part of these signaling pathways. Therefore, wild-type plants were treated with MeJa and SA, and the response of *BAT5* transcription was monitored using real-time RT-PCR. As shown in Figure 8B, an induction of the *BAT5* transcript could be observed within 5 to 120 min of application of MeJa, and levels returned to basic levels within 24 h. Conversely, treatment with SA caused an opposite effect and led to decreased steady state *BAT5* mRNA levels within 5 and 15 min (Figure 8C).

MTOB Transport Experiments

We have intensely tried to directly assess the transport characteristics of *BAT5* by measuring the transport of [³⁵S]-labeled MTOB (prepared as described in Ogier et al., 1993) into chloro-

plasts from wild-type and *bat5* mutant plants. *Arabidopsis* chloroplasts were isolated according to Kunst et al. (1988) and used for transport studies in silicone oil filtering centrifugation experiments (Fliege et al., 1978). *BAT5* was also expressed in various heterologous and homologous systems, namely, in *Escherichia coli*, yeast cells, and plant leaves. Membranes isolated from these systems and/or the recombinant transporter purified using the His-Tag system were reconstituted into artificial membranes prepared from acetone-washed soybean (*Glycine max*) phospholipids to assess transport characteristics (Loddenkötter et al., 1993). Unfortunately, all these experiments failed, most probably due to the hydrophobicity of the 2-keto acids, which leads to unspecific membrane binding and permeation, thus covering specific transport events. It therefore appears generally not feasible to directly measure transport of these substrates.

Feeding of *bat5* Mutant Plants with Various Met-Derived Intermediates Indicates That *BAT5* Is a Chloroplastic Transporter of Short- and Long-Chain 2-Keto Acids

To gain information on the transport characteristics of *BAT5*, feeding experiments were performed with *bat5* and Col-0 wild-type plants using Met-derived 2-keto acids and amino acids of different chain length. The starting molecule for the biosynthesis

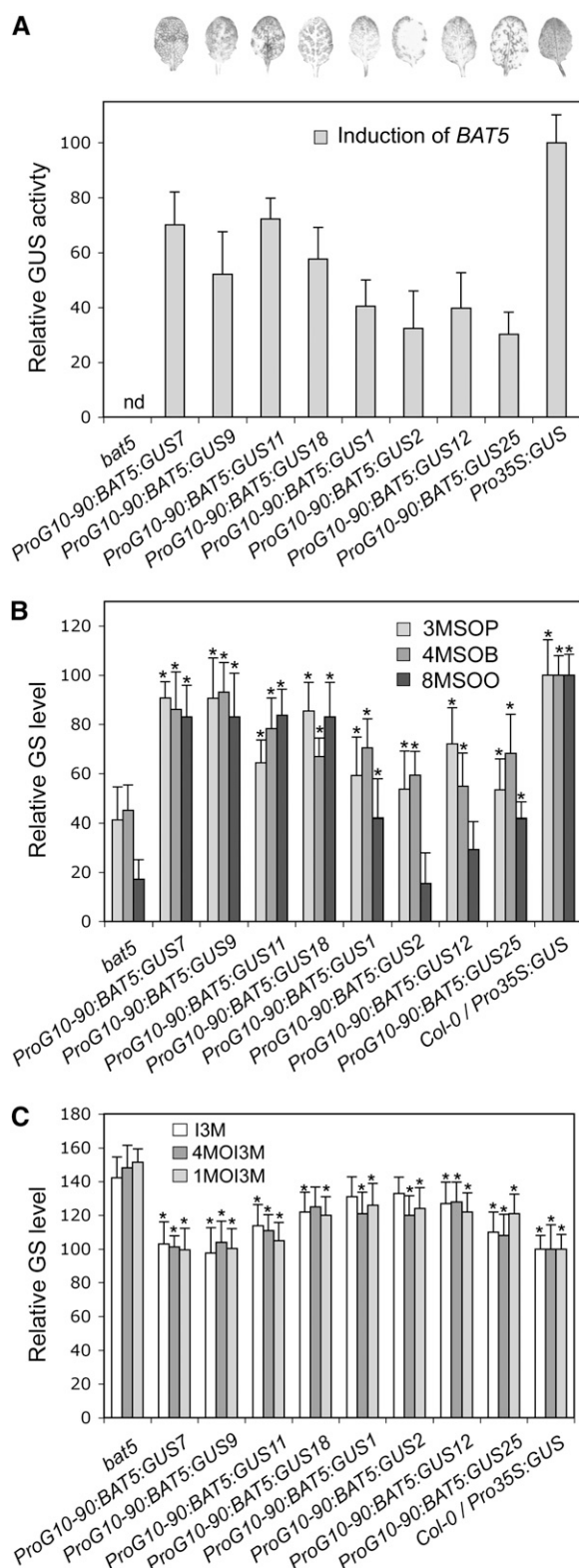


Figure 7. Gene Complementation Analysis of *bat5* Mutant Plants Using an Inducible Promoter *BAT5* Construct Fused to the *GUS* Gene.

Relative GUS activity values (**A**) and levels of aliphatic (**B**) and indolic (**C**)

of Met-derived GSs in the cytosol is the transamination product of Met, MTOB, which has to be imported into chloroplasts. *BAT5* could thus function as an importer of MTOB, and we therefore first performed feeding experiments with both MTOB and Met. On the other hand, 2-keto acids, which are chain-elongated in chloroplasts by MAM1 or MAM3, could be further transaminated either in the chloroplasts by the plastidic BCAT3 (Knill et al., 2008) or, following export of the corresponding 2-keto acid, in the cytosol by BCAT4 or yet unknown BCATs (Schuster et al., 2006; Knill et al., 2008) before being converted to aliphatic GSs. However, chain-elongated 2-keto acids or amino acids could also reenter the chloroplasts for additional side chain elongation reactions. We therefore also fed *bat5* and wild-type plants with the chain-elongated 2-keto acid MTOP, which is converted to the C3 GS 3MSOP and, in addition, with 6-methylthio-2-oxohexanoate (MTOH) and the chain-elongated amino acid dihomomethionine, which both give rise to the C4 GS, 4MSOB (Figure 9A).

As shown in Figures 9B to 9E, feeding with all three 2-keto acids (MTOB, MTOP, and MTOH) caused a drastic increase in the content of both short- and long-chain aliphatic GSs in wild-type plants. These increases can be attributed to the successful incorporation of the fed substances into the GS structure, which would imply entry of the 2-keto acids into plastids, several (maximum of six) side chain elongation reactions, and exit from the chloroplasts as chain-elongated 2-keto acids or amino acids. Remarkably, and in contrast with wild-type plants, the content of both short- and long-chain aliphatic GSs remained almost unaltered in the *bat5* mutant after feeding with MTOB. This observation indicates that *bat5* is impaired in the transport of MTOB into chloroplasts.

As also shown in Figures 9B to 9E, feeding of wild-type plants with MTOP and MTOH resulted in elevated levels of all measured aliphatic GSs. By contrast, the *bat5* mutant showed generally only a significant increase in the GS that is a direct derivative of the corresponding 2-keto acid. For example, feeding of the *bat5* mutant with MTOP resulted in an approximately eightfold increased level of 3MSOP and feeding with MTOH in five times higher levels of 4MSOB compared with *bat5* (Figures 9B to 9E). The increased synthesis of 3MSOP and 4MSOB in the *bat5* mutant is due to the fact that these aliphatic GSs can be directly synthesized in the cytosol from the corresponding 2-keto acids MTOP and MTOH (i.e., they can be transaminated by cytosolic BCATs and thus bypass transport into plastids and subsequent side chain elongation reactions). The slight increase in the levels of some long-chain aliphatic GSs in response to MTOP and MTOH feeding could be explained by the remaining *BAT5* transcript present in *bat5* plants (Figure 5A) that could support a residual uptake of 2-keto acids into plastids. Alternatively, because the uptake of 2-keto acids is impaired due to a defect in *BAT5*, they could be transaminated in the cytosol by BCATs into the corresponding amino acids, which are then transported into the plastids via a yet unknown amino acid transporter and

GSs after induction with β -estradiol are shown. Wild-type levels were set to 100%. Asterisk indicates significant difference (Student's *t* test, $P < 0.05$) in complemented lines compared with the *bat5* mutant.

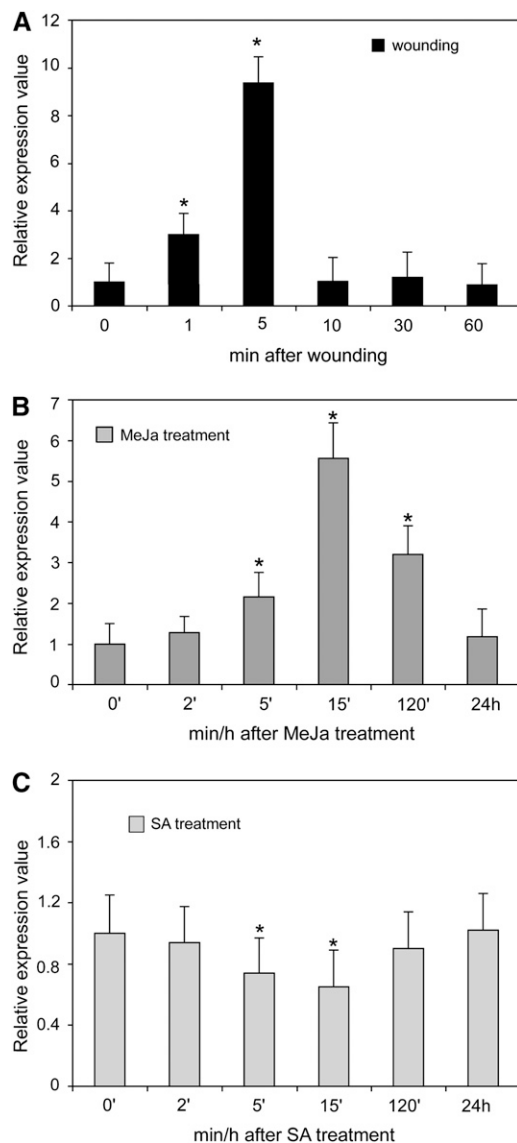


Figure 8. Induction of *BAT5* Expression by Wounding, MeJA, and SA.

(A) Wounding experiments. The plant material (inflorescences) were punctured and, after times indicated, used for real-time RT-PCR experiments (means \pm SD, $n = 3$). Relative expression values are given compared with nonwounded tissue (=1). For details, see Methods.

(B) and **(C)** Hormone experiments. Three-week-old seedlings were exposed in aqueous solutions to 10 μ M MeJA **(B)** or SA **(C)**. Samples were taken after 0, 2, 5, 10, 15, and 120 min and 24 h (means \pm SD, $n = 3$). Relative gene expression values are shown compared with noninduced plants (noninduced = 1). Asterisk indicates significant difference (Student's t test; $P < 0.05$) in comparison to the noninduced tissue.

deaminated by BCAT3 before entering the side chain elongation cycle.

Finally, feeding with Met also led to elevated levels of short- and long-chain aliphatic GSs in wild-type plants, but not in the *bat5* mutant, thus nicely corroborating observations obtained by feeding with 2-keto acids. Additionally, feeding with the chain-

elongated amino acid dihomomethionine, the transamination product of MTOH, which could directly and without additional transamination be directed into the cytosolic aliphatic GS biosynthetic pathway, also led to threefold elevated levels of 4MSOB in the *bat5* mutant (Figures 9F to 9I). The level of 4MSOB in *bat5* was even 25% higher than in the wild type, as all dihomomethionine taken up by *bat5* could only be converted into 4MSOB but to a lesser extent into longer-chained GSs. Surprisingly, not only 4MSOB, but also the 3MSOP level was moderately increased in the *bat5* mutant, which could probably be explained by a metabolic jam in the side chain elongation reaction of endogenously produced MTOH and homomethionine. If the long-chain amino acid dihomomethionine or the 2-keto acid MTOH is supplied externally, endogenously generated MTOH could not be further metabolized into long-chain 2-keto acids.

It should be noted that the feeding experiments had no significant effect on the production of indolic GSs (see Supplemental Figure 4 online). However, in all feeding experiments, the production of aliphatic GSs was significantly higher in wild-type plants than in *bat5* (Figure 9). In summary, we conclude that the *bat5* mutant is defective in the transport of 2-keto acids across the chloroplast envelope membrane.

DISCUSSION

Chloroplastidic *IPMI1*, *IPMI2*, *IPMDH1*, and *BAT5* Are Involved in the Met Side Chain Elongation of GSs

The biosynthetic pathway leading to Met-derived aliphatic GSs is highly compartmentalized and requires the participation of plastids for chain elongation reactions of corresponding 2-keto acids. These plastidic reactions include the condensation of the transaminated amino acid with acetyl-CoA, catalyzed by MAM enzymes, the isomerization of the resulting 2-alkylmalic acid to yield a 3-alkylmalic acid, and the subsequent oxidative decarboxylation to a chain-elongated 2-keto acid (Figure 10). Here, we show that the *IPMI1* and *IPMI2* isomerases and *IPMDH1*, which catalyzes the oxidative decarboxylation step, are plastid localized and are targets of *HAG1/MYB28*, the key regulator of the aliphatic GS biosynthetic pathway (Figures 1 and 4). *BAT5*, a member of the putative bile acid transporter family (Figures 1 and 4), is also a target of *HAG1/MYB28*. These findings indicate that *IPMI1*, *IPMI2*, *IPMDH1*, and *BAT5* are involved in the biosynthesis of aliphatic GSs and that the final product of MAM-mediated condensation, *IPMI1/2*-mediated isomerization, and *IPMDH1*-mediated oxidative decarboxylation are exported from the chloroplasts. The observation that *IPMI3*, *IPMDH2*, and *IPMDH3* as well as the other members of the *BAT* family (*BAT1* to *BAT4*) are not regulated by *HAG1/MYB28* suggests that these paralogs (<http://aramemnon.botanik.uni-koeln.de/>) are components of alternative pathways.

The chain-elongated 2-keto acids are further transaminated to the corresponding amino acids. It has recently been demonstrated that plastid-located BCAT3 converts MTOH and MTOH into the corresponding amino acids homomethionine and dihomomethionine (Knill et al., 2008). As shown in Figure 1, plastidic

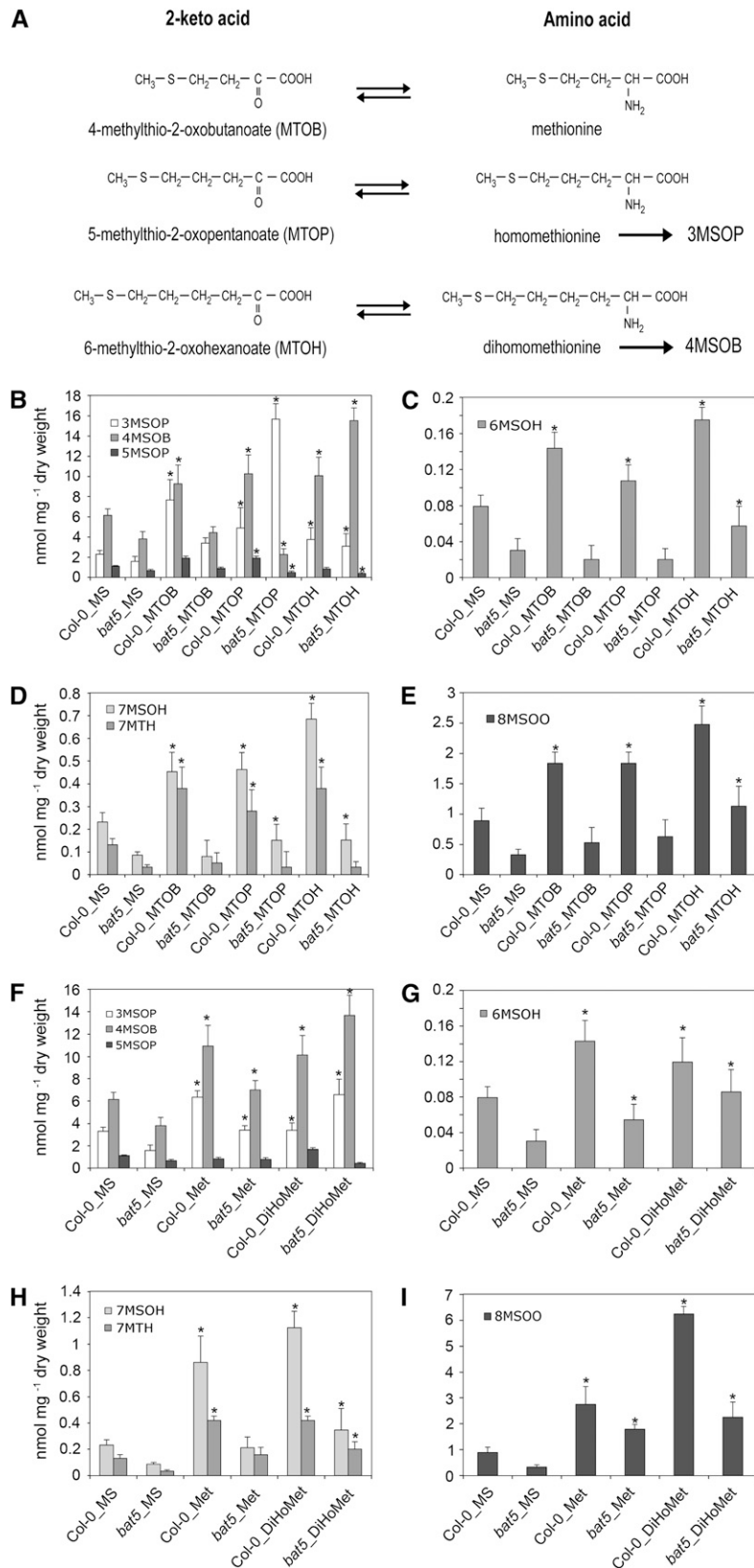


Figure 9. Metabolite Complementation Analysis of the *bat5* Mutant.

BCAT3 and cytosolic BCAT4 are targets of HAG1/MYB28. It is therefore conceivable that the 2-keto acids could be transaminated by BCATs before being imported into the plastids, as well as after being exported into the cytosol for further conversion into aliphatic GSs (Figure 10).

Generation of Met-Derived GSs Is Impaired in the *bat5* Mutant and *Pro35S:amiBAT5* Lines

In the *bat5* mutant, the level of total aliphatic GSs was not completely abolished (Figure 5B) but reduced to 50% of the wild-type level. The remaining *BAT5* transcript (Figure 5A) seems to maintain a certain level of side chain elongation and GS biosynthesis. A conceivable functional redundancy by other members of the BAT family (i.e., *BAT3* and *BAT4*) could be excluded (Figure 6). Thus, *BAT5* is the main player involved in side chain elongation reactions of Met/MTOB in chloroplasts. In addition, cultured *Pro35S:amiBAT5* cells contained 75 to 80% reduced levels of aliphatic GSs and completely abolished levels of the main aliphatic GS 4MSOB (Figure 5C). The complete absence of 4MSOB in *Pro35S:amiBAT5* cultured root cells (Figure 5E), which show a lower rate of GS biosynthesis compared with leaves (Brown et al., 2003), further supports the assumption that *BAT5* is the only BAT family member involved in the biosynthesis of Met-derived GSs in *Arabidopsis*. In addition, stably transformed *Pro35S:amiBAT5* lines (*Pro35S:amiBAT5-1*, *-7*, and *-14*) also contained reduced levels of aliphatic GSs (Figure 5D), thus corroborating the assumption that *BAT5* functions as a transporter of GS biosynthesis intermediates.

Interestingly, the *bat5* mutant does not only contain reduced levels of aliphatic GSs, but also slightly increased levels of indolic GSs (Figure 5B). This observation could be explained by the previously reported reciprocal negative feedback regulation of the two branches of aliphatic and indolic GS biosynthesis (Grubb and Abel, 2006; Gigolashvili et al., 2008). Remarkably, the increased level of indolic GSs in the *bat5* mutant could be reverted to wild-type levels in complementation experiments using the inducible vector system (Figure 7C). Interestingly, both *Pro35S:amiBAT5* transient cultured lines and stably transformed plants contained not only decreased levels of aliphatic, but also of indolic GSs. This observation could be a side effect of the *amiRNA* construct and suggests that the artificial *BAT5* *amiRNA* does not only down-regulate the expression of *BAT5* but also initiates the repression of indolic GS biosynthesis, most probably by the negative regulation of MYB34 in *BAT5* *amiRNA* plants but not in *bat5* plants (see

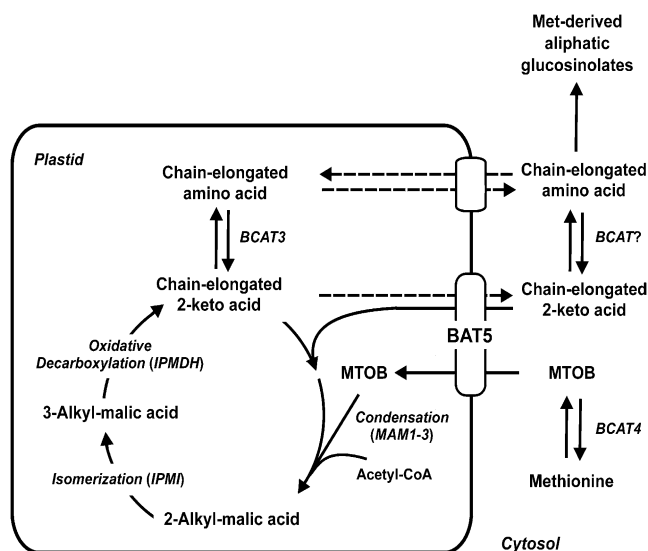


Figure 10. Schematic Representation of the Role of *BAT5* in the Transport of 2-Keto Acids, Side Chain Elongation of 2-Keto Acids, and Biosynthesis of Met-Derived GSs.

BAT5 mediates the transport of MTOB and of chain-elongated 2-keto acids. Dotted lines indicate proposed functions yet lacking experimental evidence. For details, see text.

Supplemental Figure 3 online). MYB34 was shown to be coregulated with HAG1/MYB28 (Malitsky et al., 2008), which is also repressed in *Pro35S:amiBAT5* and *bat5* lines.

Overall, the data indicate that *BAT5* is a key component in the biosynthesis of Met-derived GSs and is essential for the generation of aliphatic GSs.

BAT5 Is Active at the Site of Aliphatic GS Biosynthesis and Is Induced by Wounding and MeJa

Further evidence for *BAT5* being involved in aliphatic GS biosynthesis is provided by the tissue-specific expression pattern of *BAT5*, which overlaps with those of aliphatic GS biosynthetic genes (Figure 3; *CYP79F1* and *CYP79F2*; Reintanz et al., 2001; *BCAT4*, Schuster et al., 2006) and aliphatic GS regulators (Gigolashvili et al., 2007, 2008). *BAT5* expression was present not only in the mesophyll of leaves and the vasculature, in generative plant organs like inflorescences, flowers, and siliques, but

Figure 9. (continued).

(A) Met-derived amino acids and the corresponding 2-keto acids. Chain-elongation of 2-keto acids proceeds in plastids, and the transamination reactions are catalyzed by BCATs. Homomethionine/MTOP and dihomomethionine/MTOH are converted to the Met-derived GSs 3MSOP and 4MSOB, respectively.

(B) to (I) Two-week-old seedlings were fed with 2-keto acids or amino acids on MS plates. Feeding was performed with MTOB, MTOP, and MTOH (**(B)** to **(E)**) and Met and dihomomethionine (DiHoMet) (**(F)** to **(I)**). Means \pm SD ($n = 5$). Contents of short- and long-chained aliphatic GSs (3MSOP, 4MSOB, 5MSOP, 6MSOH, 7MSOH, 7MTH, and 8MSOO) are given in nmol/mg dry weight in comparison with Col-0. Asterisk indicates significant difference in comparison to the wild type or *bat5*, respectively (Student's *t* test, $P < 0.05$). Plants were germinated on half-strength Murashige and Skoog (MS) plates with agar, and 2-week-old wild-type and *bat5* seedlings were transferred to media supplemented with 0.2 mM MTOB, MTOP, MTOH, Met, or dihomomethionine, respectively, for 14 additional days, followed by analyses of aliphatic GSs.

also in nonphotosynthetic organs like roots (i.e., at sites where aliphatic GSs are found) (Brown et al., 2003). Environmental stimuli, such as wounding, which are known to have an impact on GS biosynthesis also affected *BAT5* expression (Figure 8). Consistent with the wound-induced mRNA accumulation of aliphatic GS regulators (HAG1/MYB28, HAG3/MYB29, and HAG2/MYB76), *BAT5* transcript levels increased up to ninefold 5 min after wounding (Figure 8A). Several GS biosynthetic pathway genes like *MAM1*, *BCAT4*, *BCAT3*, and *CYP79F1* were also shown to be induced upon mechanical stimuli (Schuster et al., 2006; Gigolashvili et al., 2007; Knill et al., 2008). Furthermore, we demonstrated that *BAT5* expression is induced in response to MeJa (Figure 8B) and repressed after SA treatment (Figure 8C), consistent with the increased accumulation of aliphatic GSs (5MSOP and 8MSOO) and the observation that the aliphatic GS regulator, HAG3/MYB29, is upregulated in response to MeJa (Hirai et al., 2007; Gigolashvili et al., 2008) and repressed by SA treatment (Gigolashvili et al., 2008). Thus, *BAT5* is a target of the main regulators of aliphatic GS biosynthesis (Figure 1) and appears to integrate the different environmental cues, as has been shown for HAG1/MYB28, HAG2/MYB76, and HAG3/MYB29.

BAT5 Is Involved in the Transport of MTOB and of Chain-Elongated 2-Keto Acids

Besides the observations that *BAT5* expression closely correlates with that of other Met-derived GS biosynthetic genes, such as *MAM3*, *CYP79F1*, *CYP79F2*, *BCAT4*, *BCAT3*, and *St5b*, and that *BAT5* is a target for three main aliphatic GS regulators HAG1/MYB28, HAG3/MYB29, and HAG2/MYB76 (Table 1, Figure 1), several lines of evidence indicate a role for the plastidic *BAT5* in the chain-elongation pathway of Met-derived GS biosynthesis and, particularly, in the transport of short- and long-chain 2-keto acids (Figure 10). First, the reduced levels of aliphatic GSs in the *bat5* mutant could not be rescued by feeding with MTOB or Met. By contrast, external MTOB or Met supply to wild-type plants caused a considerable increase in the accumulation of Met-derived GSs (Figures 9B to 9E). The observation that MTOB and Met feeding did not rescue the *bat5* mutant chemotype indicates that the import of Met via an amino acid transporter or of MTOB, the BCAT4-mediated transamination product, via a 2-keto acid transporter is impaired in *bat5*. Assuming that *BAT5* represents an amino acid transporter, MTOB feeding should result in wild-type levels of GSs, since MTOB could be taken up, chain-elongated, and exported as chain-elongated 2-keto acid for further conversion into GSs. This is, however, not the case. On the other hand, if *BAT5* represents a 2-keto acid transporter affected in *bat5*, the fed MTOB could be transaminated to Met and imported into chloroplasts for transamination and chain elongation reactions resulting also in aliphatic GS levels similar to those in the wild type. This is also not the case, strongly suggesting that (1) Met is generally only poorly taken up by plastids for GS biosynthesis and (2) that *BAT5* most probably represents a transporter for MTOB and other 2-keto acids.

Likewise, because Met, if not transaminated into MTOB, represents only a poor substrate for GS biosynthesis, it could, however, in Met-feeding experiments be transaminated to MTOB and subsequently be taken up and exported as chain-

elongated 2-keto acid, thereby resulting in increased accumulation of aliphatic GSs. This actually also does not hold true in *bat5*, again indicating that *BAT5* represents a transporter for MTOB and chain-elongated 2-keto acids. The slight overall increase in aliphatic GSs in the *bat5* mutant in feeding experiments with MTOB and Met can be assigned to the residual activity of *BAT5* and not to redundant *BAT* activities because the double *bat5 bat4* and the triple *bat5 bat4 bat3* mutant phenocopy the single *bat5* mutant (Figure 6).

Second, MTOB feeding restored the reduced level of 3MSOP in the *bat5* mutant. Likewise, the reduced level of 4MSOB could be rescued by feeding with MTOH and dihomomethionine but not with MTOB, demonstrating that (1) the cytosolic conversion of 2-keto acids into corresponding amino acids proceeds very efficiently and (2) that bypassing the plastidic *BAT5* function directly led to the biosynthesis of aliphatic GSs (Figures 9 and 10). Third, feeding with MTOB, MTOH, or dihomomethionine led to elevated levels of the long-chained aliphatic GSs 6MSOH, 7MSOH, 7MTH, and 8MSOO only in wild-type plants but not in the *bat5* mutant. This indicates that the chain-elongated 2-keto acids MTOB and MTOH could only be imported into chloroplasts in the wild type but not in the *bat5* mutant, again demonstrating a function of *BAT5* in the transport of chain-elongated 2-keto acids. Also, the observation that MTOH-supplemented *bat5* plants contained lower levels of long-chain aliphatic GSs than dihomomethionine-supplemented plants (Figures 9B to 9I) supports the suggestion that *BAT5* is a transporter of 2-keto acids, but not of amino acids. Altogether, the experimental evidence strongly suggests that *BAT5* mediates the transport of MTOB and of long-chain 2-keto acids. It is also apparent from these experiments that the fed 2-keto acids and amino acids can enter the long-distance transport pathway, including transport across plasma and plastidic membranes, and that the transport across the plastidic membrane is impaired in the *bat5* mutant.

The combined data suggest that *BAT5* transports MTOB and chain-elongated 2-keto acids across the chloroplast envelope membrane before, during, and after side chain-elongation of 2-keto acids and is thus an essential component of the aliphatic GS biosynthetic pathway.

METHODS

Plant Material and Growth Conditions

Seeds of *Arabidopsis thaliana*, ecotype Col-0, and corresponding loss-of-function mutants were plated on soil and cold-treated at 4°C for 3 d in the dark. After stratification, seeds were transferred into a temperature-controlled growth chamber under short-day conditions (8 h light, 16 h dark) at 21 to 22°C and 40% humidity. Transgenic plants were selected by germination on half-strength MS medium containing corresponding antibiotics and were subsequently treated as wild-type plants.

Phylogenetic Analysis

Homologs of human bile acid transporter presented in Figure 2 were identified using BLAST (Altschul et al., 1990). Protein sequences for all putative bile acid transporter proteins (shown in Supplemental Data Set 1 online) were aligned using the ClustalW program with default settings (<http://www-ebi.ac.uk/clustalw>) and adjusted manually. An unrooted tree

was visualized using Treeview software (<http://taxonomy.zoology.gla.ac.uk/rod/treeview.html>).

Cotransformation Assays with Cultured *Arabidopsis* Cells

Cultured *Arabidopsis* Col-0 cells were maintained in 50 mL of *Arabidopsis* (AT) medium. The AT medium contained 4.3 g/L MS basal salt media (Duchefa), 1 mg/L 2,4-D, 4 mL of a vitamin B5 mixture (Sigma-Aldrich), and 30 g/L sucrose, pH 5.8. Cells were gently agitated at 160 rpm in the dark at 22°C.

To generate reporter constructs, the promoter regions of the genes of interest (*BAT1*, *BAT2*, *BAT3*, *BAT4*, *BAT5*, *IPM11*, *IPM12*, *IMDH1*, *BCAT3*, and *MAM1*) were amplified from genomic DNA of *Arabidopsis* plants and cloned into the pTOPO entry or pDONOR-207 vector (Invitrogen Life Technologies). To drive *Agrobacterium tumefaciens*-mediated expression of the *uidA* (*GUS*) reporter gene under control of these promoters, the pGWB3i vector was recombined with the pTOPO entry or pDONOR-207 vector containing corresponding promoters sequences using LR reactions (Invitrogen Life Technologies). As an effector, a previously generated pGWB2 vector containing the full-length clone of *HAG1/MYB28*, *HAG2/MYB76*, or *HAG3/MYB76* was used (Gigolashvili et al., 2007, 2008). Finally, the reporter and effector constructs were transformed into the supervirulent *Agrobacterium* strain LBA4404.pBBR1MCS.virGN54D. Transient coexpression assays in cultured cells were performed as described by Berger et al. (2007).

Construction of the GFP Fusion Plasmids and Transfection of Cultured *Arabidopsis* Cells

To generate GFP fusion constructs, the *BAT5*, *IPM11*, *IPM12*, and *IPMDH1* coding regions, including the putative chloroplast targeting sequences, were first cloned into the entry pDONOR-207 vector. The obtained entry clones were recombined with the pGWB5 binary vector using LR reactions. Transformation of dark-grown cultured *Arabidopsis* cells was performed using supervirulent *Agrobacterium* strains LBA4404.pBBR1MCS.virGN54D each containing one of these constructs as described by Koroleva et al. (2005).

For transient expression of the full-length *BAT5* clone in *Arabidopsis* leaves, the supervirulent *Agrobacterium* containing the *BAT5-GFP* construct and the antisilencing *Agrobacterium* strain 19K were taken from fresh YEB plates, grown overnight, sedimented, resuspended in 10 mM MgCl₂ and 10 mM MES, pH 5.6, and adjusted to an OD₆₀₀ of 0.7 to 0.8. The working solutions for the infiltration of dark-exposed *Arabidopsis* plants contained a *BAT5-GFP* suspension together with the *Agrobacterium* strain 19K in a 1:1 ratio. Acetosyringon was added (0.15 mM, final concentration), and the suspension was incubated for 2 to 4 h at 30°C. Three to five leaves of 5- to 6-week-old *Arabidopsis* plants were infiltrated with the working solution and sampled after 3 to 5 d of infiltration for microscopy. GFP expression patterns were recorded using a fluorescence microscope (Eclipse E800; Nikon) with a GFP (R)-BP filter (excitation 460 to 500 nm; dichronic mirror 505 nm; barrier filter 510 to 560 nm) or a SP2 confocal laser scanning microscope from Leica. Photomicrographs were taken with Ducus and LCS software.

Generation of Transgenic *Pro35S:amiBAT5* Lines

To construct an amiRNA against *BAT5*, an artificial microRNA fragment was designed as described at <http://wmd.weigelworld.org> and cloned into the Gateway TOPO Entry vector. For amplification of the miR319a precursor, the RS300 plasmid, kindly provided by D. Weigel (Max Planck Institute for Developmental Biology, Tuebingen, Germany), was used. The obtained pTOPO Entry clone containing the *amiBAT5* sequence was recombined into the Gateway destination pGWB2 vector.

To generate *Pro35S:amiBAT5 Arabidopsis* knockdown plants and corresponding cells, *Pro35S:amiBAT5:GWB2* was transformed into the

Agrobacterium strain GV3101 and LBA4404.pBBR1MCS.virGN54D by electroporation and further into *Arabidopsis* plants and cultured cells. Plant transformants were selected with kanamycin (50 µg per mL), and the *BAT5* transcript level was monitored by real-time PCR analysis.

Generation of the Estradiol-Inducible *ProG10-90:BAT5:GUS* Construct for the Complementation Analysis

To rescue *BAT5* function, an estrogen receptor-based chemical-inducible system (Zuo et al., 2000) modified for gateway cloning by I. Somssich (Max Planck Institute for Plant Breeding Research, Cologne, Germany) was used. To generate an expression clone, the coding sequence of *BAT5* was first amplified by RT-PCR and cloned into the TOPO Entry vector (Invitrogen Life Technologies) before being recombined into the destination pMD-GWY-St vector using the LR reaction. The final *ProG10-90:BAT5:GUS* construct within the pMD-GWY-St vector was transformed into *Agrobacterium* cells by electroporation and into *Arabidopsis* plants by vacuum infiltration (Bechtold et al., 1993). All transformants were selected using BASTA, and the *uidA* transcript level was monitored by histochemical GUS staining.

Histochemical Analysis of Transgenic Plants Expressing the *ProBAT5:uidA* Fusion Construct

The promoter region of the *BAT5* gene was amplified from genomic DNA of *Arabidopsis* plants and cloned into the pTOPO Entry vector (Invitrogen Life Technologies). To drive expression of the *uidA* gene under control of the *BAT5* promoter, the binary Gateway-compatible plant transformation vector pGWB3 was recombined with the entry clone using an LR reaction. The obtained *ProBAT5:uidA* construct was transformed into the GV3101 *Agrobacterium* strain and *Arabidopsis* wild-type plants.

Histochemical localization of GUS in several independent transgenic lines harboring the *ProBAT5:uidA* construct was performed as described previously (Gigolashvili et al., 2007).

Preparation of Methanolic Extracts and HPLC Analysis of GSs

Fifty milligrams of leaves were placed into a 2-mL reaction tube and frozen in liquid nitrogen. Frozen leaf samples were lyophilized and homogenized in a mill (Qiagen). GSs were extracted in 80% methanol after addition of 20 µL of 5 mM of benzyl GS as an internal standard (www.glucosinolates.com). Extracts were applied onto a DEAE Sephadex A25 column (0.1 g powder equilibrated in 0.5 M acetic acid/NaOH, pH 5). GSs were converted to desulfoglucosinolates by overnight incubation with a purified sulfatase (E.C. 3.1.6.1) designated type H-1, from *Helix pomatia*, 16,400 units/g solid (Sigma-Aldrich). For analysis of desulfoglucosinolates, samples were subjected to UPLC analysis (Waters) with a diode array detector, using an Acquity UPLC column (BEH Schield RP18, 150 × 2.1 mm, 1.7 µm). Peaks were quantified by the peak area at 229 nm relative to the area of the internal standard peak.

Reverse Transcriptase-Mediated First-Strand Synthesis and Real-Time PCR Analysis

Total RNA was extracted from rosette leaves of adult plants from different mutant lines using the TRIsure buffer (Biolone) followed by treatment with RNase-free DNase (Roth) to remove genomic DNA contaminants. Seven-to-ten micrograms of total RNA was reverse transcribed with the first-strand cDNA synthesis SSII kit (Invitrogen) according to the manufacturer's instructions.

The expression of genes was analyzed in three independent replicates by real-time RT-PCR analysis using the fluorescent intercalating dye SYBR-Green in a GeneAmp 7300 sequence detection system (Applied Biosystems). The *Arabidopsis ACTIN2* gene was used as a standard.

Real-time PCR was performed using the SYBR-Green master kit system (Applied Biosystems) according to the manufacturer's instructions. The Ct, defined as the PCR cycle at which a statistically significant increase of reporter fluorescence is detected, is used as a measure for the starting copy number of the target gene. Relative quantification of expression levels was performed using relative quantification software based on the comparative Ct method (Applied Biosystems). The calculated relative expression values are normalized to the wild-type expression level, wild type = 1. The efficiency of each primer pair was tested using wild-type (Col-0) cDNA as a standard template, and the RT-PCR data were normalized dependent on the relative efficiency of each primer pair.

Plant Hormone Induction and Wounding Experiments

Arabidopsis wild-type seedlings (Col-0) were grown on half-strength MS media with 0.5% agar and 0.5% sucrose for 10 d in a growth chamber at 21°C under constant light. Afterwards, roots and portions of the first leaves were immersed in half-strength MS liquid media containing MeJA or SA (10 μM) and incubated for 0, 2, 5, 15, or 120 min, or for 24 h. Subsequently, the seedlings were placed into 2-mL reaction tubes, frozen in liquid nitrogen, and used for RNA isolation. Three independent sets of plants induced by this elicitor were used for real-time PCR analysis.

For wounding experiments, inflorescences of Col-0 plants were slightly cut with a scalpel or blade. Samples were collected 0, 1, 5, 10, 30, and 60 min after treatment, immediately frozen in liquid nitrogen, and used for RNA isolation and real-time PCR analysis.

Feeding Experiment with 2-Keto Acids and Amino Acids

Seedlings of the wild type (Col-0) and *bat5* mutant were grown on half-strength MS media with 1% agar and 0.5% sucrose for 14 d in a growth chamber at 21°C under short-day conditions. Afterwards, both Col-0 and *bat5* were carefully taken out of plates and transferred into six-well plates containing half-strength MS supplemented with 0.2 mM MTOB, MTOP, MTOH, Met, or dihomomethionine, respectively. Plants were left for 14 additional days under the same conditions, followed by analyses of GS contents using UPLC.

MTOB and Met were obtained from Sigma-Aldrich. MTOP and MTOH were synthesized by Applichem. Dihomomethionine was synthesized as described by Dawson et al. (1993). In short, sodium methoxide (0.033 mol) was treated with methylmercaptane, and 3-bromovaleronitrile was subsequently added to yield 5-methylthiopentenenitrile. This was converted to 5-methylthiopentanal by treatment with diisobutylaluminum hydride. The 5-methylthiopentanal was first converted into the corresponding aminonitrile and subsequently hydrolyzed to dihomomethionine, which was further purified by anion exchange chromatography.

Accession Numbers

Sequence data from this article can be found in the Arabidopsis Genome Initiative or GenBank/EMBL databases under the following accession numbers: *BAT5* (At4g12030.2, representative gene model; <http://Arabidopsis.org>), *BAT4* (At4g22840), *BAT3* (At3g25410), *BAT2* (At1g78560), *BAT1* (At2g26900), *IPM1* (At3g58990), *IPM2* (At2g43100), and *IPMDH* (At1g31180).

Supplemental Data

The following materials are available in the online version of this article.

Supplemental Figure 1. Histochemical GUS Staining in Various Tissues of *ProBAT1-4:GUS* Plants.

Supplemental Figure 2. Plastidic Localization of *BAT1*, *BAT2*, *BAT3*, and *BAT4* Full-Length GFP Constructs in BY Tobacco Protoplasts.

Supplemental Figure 3. Transcript Levels of Known Glucosinolate Biosynthesis Regulators in Leaves of *bat5* and *Pro35S:amiBAT5* Plants in Comparison with the Wild Type (Col-0).

Supplemental Figure 4. Content of the Indolic Glucosinolate Indol-3-Ylmethyl-GS in *bat5* Mutant Fed with 2-Keto Acids or Amino Acids.

Supplemental Data Set 1. Protein Sequences Used to Generate the Phylogenetic Tree Presented in Figure 2.

ACKNOWLEDGMENTS

This work was supported by the Deutsche Forschungsgemeinschaft. We thank A. Berkessel (University of Cologne, Germany) for providing facilities for the synthesis of dihomomethionine I.E. Somssich (Max Planck Institute for Plant Breeding Research, Cologne, Germany) for providing the ergosterol-inducible gateway construct, and Katja Wester for help with confocal microscopy.

Received February 18, 2009; revised May 15, 2009; accepted June 3, 2009; published June 19, 2009.

REFERENCES

- Altschul, S.F., Gish, W., Miller, W., Myers, E.W., and Lipman, D.J. (1990). Basic local alignment search tool. *J. Mol. Biol.* **215**: 403–410.
- Bechtold, N., Ellis, J., and Pelletier, G. (1993). In planta *Agrobacterium*-mediated gene transfer by infiltration of adult *Arabidopsis thaliana* plants. *C. R. Acad. Sci. Paris Life Sci.* **316**: 1194–1199.
- Berger, B., Stracke, R., Yatusevich, R., Weisshaar, B., Flügge, U.I., and Gogolashvili, T. (2007). A simplified method for the analysis of transcription factor-promoter interactions that allows high-throughput data generation. *Plant J.* **50**: 911–916.
- Brader, G., Mikkelsen, M.D., Halkier, B.A., and Palva, E.T. (2006). Altering glucosinolate profiles modulates disease resistance in plants. *Plant J.* **46**: 758–767.
- Brader, G., Tas, E., and Palva, E.T. (2001). Jasmonate-dependent induction of indole glucosinolates in *Arabidopsis* by culture filtrates of the nonspecific pathogen *Erwinia carotovora*. *Plant Physiol.* **126**: 849–860.
- Brown, P.D., Tokuhisa, J.G., Reichelt, M., and Gershenzon, J. (2003). Variation of glucosinolate accumulation among different organs and developmental stages of *Arabidopsis thaliana*. *Phytochemistry* **62**: 471–481.
- Chen, S.X., Glawischignig, E., Jorgensen, K., Naur, P., Jorgensen, B., Olsen, C.E., Hansen, C.H., Rasmussen, H., Pickett, J.A., and Halkier, B.A. (2003). CYP79F1 and CYP79F2 have distinct functions in the biosynthesis of aliphatic glucosinolates in *Arabidopsis*. *Plant J.* **33**: 923–937.
- Chung, W.C., Huang, H.C., Chiang, B.T., Huang, H.C., and Huang, J.W. (2005). Inhibition of soil-borne plant pathogens by the treatment of sinigrin and myrosinases released from reconstructed *Escherichia coli* and *Pichia pastoris*. *Biocontrol Sci. Technol.* **15**: 455–465.
- Cipollini, D., Enright, S., Traw, M.B., and Bergelson, J. (2004). Salicylic acid inhibits jasmonic acid-induced resistance of *Arabidopsis thaliana* to *Spodoptera exigua*. *Mol. Ecol.* **13**: 1643–1653.
- Dawson, G.W., Hick, A.J., Bennett, R.N., Donald, A., Pickett, J.A., and Wallsgrove, R.M. (1993). Synthesis of glucosinolate precursors and investigations into the biosynthesis of phenylalkyl- and methylthioalkylglucosinolates. *J. Biol. Chem.* **268**: 27154–27159.

- Devoto, A., and Turner, J.G.** (2005). Jasmonate-regulated Arabidopsis stress signalling network. *Physiol. Plant.* **123**: 161–172.
- Fliege, R., Flügge, U.I., Werdan, K., and Heldt, H.W.** (1978). Specific transport of inorganic phosphate, 3-phosphoglycerate and triose-phosphates across the inner membrane of the envelope in spinach chloroplasts. *Biochim. Biophys. Acta* **502**: 232–247.
- Giamoustaris, A., and Mithen, R.** (1995). The effect of modifying the glucosinolate content of leaves of oilseed rape (*Brassica Napus Ssp Oleifera*) on its interaction with specialist and generalist pests. *Ann. Appl. Biol.* **126**: 347–363.
- Gigolashvili, T., Engqvist, M., Yatusевич, R., Müller, C., and Flügge, U.I.** (2008). HAG2/MYB76 and HAG3/MYB29 exert a specific and coordinated control on the regulation of aliphatic glucosinolate biosynthesis in *Arabidopsis thaliana*. *New Phytol.* **177**: 627–642.
- Gigolashvili, T., Berger, B., Mock, H.P., Müller, C., Weisshaar, B., and Flügge, U.I.** (2007a). The transcription factor HIG1/MYB51 regulates indolic glucosinolate biosynthesis in *Arabidopsis thaliana*. *Plant J.* **50**: 886–901.
- Gigolashvili, T., Yatusевич, R., Berger, B., Müller, C., and Flügge, U.I.** (2007b). The R2R3-MYB transcription factor HAG1/MYB28 is a regulator of methionine-derived glucosinolate biosynthesis in *Arabidopsis thaliana*. *Plant J.* **51**: 247–261.
- Grubb, C.D., and Abel, S.** (2006). Glucosinolate metabolism and its control. *Trends Plant Sci.* **11**: 89–100.
- Grubb, C.D., Zipp, B.J., Ludwig-Muller, J., Masuno, M.N., Molinski, T.F., and Abel, S.** (2004). Arabidopsis glucosyltransferase UGT74B1 functions in glucosinolate biosynthesis and auxin homeostasis. *Plant J.* **40**: 893–908.
- Hagenbuch, B., Stieger, B., Foguet, M., Lubbert, H., and Meier, P.J.** (1991). Functional expression cloning and characterization of the hepatocyte Na⁺/bile acid cotransport system. *Proc. Natl. Acad. Sci. USA* **88**: 10629–10633.
- Halkier, B.A., and Gershenzon, J.** (2006). Biology and biochemistry of glucosinolates. *Annu. Rev. Plant Biol.* **57**: 303–333.
- Hansen, C.H., Wittstock, U., Olsen, C.E., Hick, A.J., Pickett, J.A., and Halkier, B.A.** (2001). Cytochrome P450 CYP79F1 from Arabidopsis catalyzes the conversion of dihomomethionine and trihomomethionine to the corresponding aldoximes in the biosynthesis of aliphatic glucosinolates. *J. Biol. Chem.* **276**: 11078–11085.
- Hayes, D., Kelleher, O., and Eggelston, M.** (2008). The cancer chemoprotective actions of phytochemicals derived from glucosinolates. *Eur. J. Nutr.* **47** (Suppl. 2): 73–88.
- Hemm, M.R., Ruegger, M.O., and Chapple, C.** (2003). The Arabidopsis *ref2* mutant is defective in the gene encoding CYP83A1 and shows both phenylpropanoid and glucosinolate phenotypes. *Plant Cell* **15**: 179–194.
- Hirai, M.Y., et al.** (2007). Omics-based identification of Arabidopsis Myb transcription factors regulating aliphatic glucosinolate biosynthesis. *Proc. Natl. Acad. Sci. USA* **104**: 6478–6483.
- Kliebenstein, D.J., Kroymann, J., Brown, P., Figuth, A., Pedersen, D., Gershenzon, J., and Mitchell-Olds, T.** (2001). Genetic control of natural variation in Arabidopsis glucosinolate accumulation. *Plant Physiol.* **126**: 811–825.
- Knill, T., Schuster, J., Reichelt, M., Gershenzon, J., and Binder, S.** (2008). Arabidopsis branched-chain aminotransferase 3 functions in both amino acid and glucosinolate biosynthesis. *Plant Physiol.* **146**: 1028–1039.
- Koroleva, O.A., Tomlinson, M.L., Leader, D., Shaw, P., and Doonan, J.H.** (2005). High-throughput protein localization in Arabidopsis using Agrobacterium-mediated transient expression of GFP-ORF fusions. *Plant J.* **41**: 162–174.
- Kroymann, J., Textor, S., Tokuhisa, J.G., Falk, K.L., Bartram, S., Gershenzon, J., and Mitchell-Olds, T.** (2001). A gene controlling variation in Arabidopsis glucosinolate composition is part of the methionine chain elongation pathway. *Plant Physiol.* **127**: 1077–1088.
- Kunst, L., Browse, J., and Somerville, C.** (1988). Altered regulation of lipid biosynthesis in a mutant of *Arabidopsis* deficient in chloroplast glycerol-3-phosphate acyltransferase activity. *Proc. Natl. Acad. Sci. USA* **85**: 4143–4147.
- Li, J., Hansen, B.G., Ober, J.A., Kliebenstein, D.J., and Halkier, B.A.** (2008). Subclade of flavin-monooxygenases involved in aliphatic glucosinolate biosynthesis. *Plant Physiol.* **148**: 1721–1733.
- Loddenkötter, B., Kammerer, B., Fischer, K., and Flügge, U.I.** (1993). Expression of the functional mature chloroplast triose phosphate translocator in yeast internal membranes and purification of the histidine-tagged protein by a single metal-affinity chromatography step. *Proc. Natl. Acad. Sci. USA* **90**: 2155–2159.
- Malitsky, S., Blum, E., Less, H., Venger, I., Elbaz, M., Morin, S., Eshed, Y., and Aharoni, A.** (2008). The transcript and metabolite networks affected by the two clades of Arabidopsis glucosinolate biosynthesis regulators. *Plant Physiol.* **148**: 2021–2049.
- Manici, L.M., Lazzeri, L., Baruzzi, G., Leoni, O., Galletti, S., and Palmieri, S.** (2000). Suppressive activity of some glucosinolate enzyme degradation products on *Pythium irregulare* and *Rhizoctonia solani* in sterile soil. *Pest Manag. Sci.* **56**: 921–926.
- Mari, M., Iori, R., Leoni, O., and Marchi, A.** (1996). Bioassays of glucosinolate-derived isothiocyanates against postharvest pear pathogens. *Plant Pathol.* **45**: 753–760.
- Mewis, I., Appel, H.M., Hom, A., Raina, R., and Schultz, J.C.** (2005). Major signaling pathways modulate Arabidopsis glucosinolate accumulation and response to both phloem-feeding and chewing insects. *Plant Physiol.* **138**: 1149–1162.
- Mikkelsen, M.D., and Halkier, B.A.** (2003). Metabolic engineering of valine- and isoleucine-derived glucosinolates in Arabidopsis expressing CYP79D2 from cassava. *Plant Physiol.* **131**: 773–779.
- Mikkelsen, M.D., Naur, P., and Halkier, B.A.** (2004). Arabidopsis mutants in the C-S lyase of glucosinolate biosynthesis establish a critical role for indole-3-acetaldoxime in auxin homeostasis. *Plant J.* **37**: 770–777.
- Mithen, R.F.** (2001). Glucosinolates and their degradation products. *Adv. Bot. Res.* **35**: 213–262.
- Mugford, S.G., et al.** (2009). Disruption of adenosine-5'-phosphosulfate kinase in *Arabidopsis* reduces levels of sulfated secondary metabolites. *Plant Cell* **21**: 910–927.
- Naur, P., Petersen, B.L., Mikkelsen, M.D., Bak, S., Rasmussen, H., Olsen, C.E., and Halkier, B.A.** (2003). CYP83A1 and CYP83B1, two nonredundant cytochrome P450 enzymes metabolizing oximes in the biosynthesis of glucosinolates in Arabidopsis. *Plant Physiol.* **133**: 63–72.
- Ogier, G., Chantepie, J., Deshayes, C., Chantegrel, B., Charlot, C., Doutheau, A., and Quash, G.** (1993). Contribution of 4-methylthio-2-oxobutanoate and its transaminase to the growth of methionine-dependent cells in culture. Effect of transaminase inhibitors. *Biochem. Pharmacol.* **45**: 1631–1644.
- Piotrowski, M., Schemenewitz, A., Lopukhina, A., Müller, A., Janowitz, T., Weiler, E.W., and Oecking, C.** (2004). Desulfoglucosinolate sulfotransferases from *Arabidopsis thaliana* catalyze the final step in the biosynthesis of the glucosinolate core structure. *J. Biol. Chem.* **279**: 50717–50725.
- Price, C.E., Reid, S.J., Driessen, A.J.M., and Abratt, V.R.** (2006). The *Bifidobacterium longum* NCIMB 702259^T *ctr* gene codes for a novel cholate transporter. *Appl. Environ. Microbiol.* **72**: 923–926.
- Reintanz, B., Lehnen, M., Reichelt, M., Gershenzon, J., Kowalczyk, M., Sandberg, G., Godde, M., Uhl, R., and Palme, K.** (2001). *bus*, a bushy Arabidopsis CYP79F1 knockout mutant with abolished synthesis of short-chain aliphatic glucosinolates. *Plant Cell* **13**: 351–367.

- Reymond, P., Bodenhausen, N., Van Poecke, R.M.P., Krishnamurthy, V., Dicke, M., and Farmer, E.E.** (2004). A conserved transcript pattern in response to a specialist and a generalist herbivore. *Plant Cell* **16**: 3132–3147.
- Rzewuski, G., and Sauter, M.** (2002). The novel rice (*Oryza sativa* L.) gene *OsSbf1* encodes a putative member of the Na⁺/bile acid symporter family. *J. Exp. Bot.* **53**: 1991–1993.
- Sasaki-Sekimoto, Y., et al.** (2005). Coordinated activation of metabolic pathways for antioxidants and defence compounds by jasmonates and their roles in stress tolerance in *Arabidopsis*. *Plant J.* **44**: 653–668.
- Schuster, J., Knill, T., Reichelt, M., Gershenzon, J., and Binder, S.** (2006). BRANCHED-CHAIN AMINOTRANSFERASE4 is part of the chain elongation pathway in the biosynthesis of methionine-derived glucosinolates in *Arabidopsis*. *Plant Cell* **18**: 2664–2679.
- Schwab, R., Ossowski, S., Riester, M., Warthmann, N., and Weigel, D.** (2006). Highly specific gene silencing by artificial microRNAs in *Arabidopsis*. *Plant Cell* **18**: 1121–1133.
- Schwacke, R., Schneider, A., van der Graaff, E., Fischer, K., Catoni, E., Desimone, M., Frommer, W.B., Flügge, U.I., and Kunze, R.** (2003). ARAMEMNON: A novel database for *Arabidopsis thaliana* integral membrane proteins. *Plant Physiol.* **131**: 16–26.
- Sønderby, I.E., Hansen, B.G., Bjarnholt, N., Ticconi, C., Halkier, B.A., and Kliebenstein, D.J.** (2007). A systems biology approach identifies a R2R3 MYB gene subfamily with distinct and overlapping functions in regulation of aliphatic glucosinolates. *PLoS One* **2**: e1322.
- Talalay, P., and Fahey, J.W.** (2001). Phytochemicals from cruciferous plants protect against cancer by modulating carcinogen metabolism. *J. Nutr.* **131**: 3027S–3033S.
- Tantikanjana, T., Mikkelsen, M.D., Hussain, M., Halkier, B.A., and Sundaresan, V.** (2004). Functional analysis of the tandem-duplicated P450 genes *SPS/BUS/CYP79F1* and *CYP79F2* in glucosinolate biosynthesis and plant development by Ds transposition-generated double mutants. *Plant Physiol.* **135**: 840–848.
- Textor, S., Bartram, S., Kroymann, J., Falk, K.L., Hick, A., Pickett, J. A., and Gershenzon, J.** (2004). Biosynthesis of methionine-derived glucosinolates in *Arabidopsis thaliana*: Recombinant expression and characterization of methylthioalkylmalate synthase, the condensing enzyme of the chain-elongation cycle. *Planta* **218**: 1026–1035.
- Textor, S., de Kraker, J.W., Hause, B., Gershenzon, J., and Tokuhisa, J.G.** (2007). MAM3 catalyzes the formation of all aliphatic glucosinolate chain lengths in *Arabidopsis*. *Plant Physiol.* **144**: 60–71.
- Trauner, M., and Boyer, J.L.** (2003). Bile salt transporters: molecular characterization, function, and regulation. *Physiol. Rev.* **83**: 633–671.
- Traw, M.B., Kim, J., Enright, S., Cipollini, D.F., and Bergelson, J.** (2003). Negative cross-talk between salicylate- and jasmonate-mediated pathways in the *Wassilewskija* ecotype of *Arabidopsis thaliana*. *Mol. Ecol.* **12**: 1125–1135.
- Wong, M.H., Oelkers, P., Craddock, A.L., Dawson, P.A.** (1994). Expression cloning and characterization of the hamster ileal sodium-dependent bile acid transporter. *J. Biol. Chem.* **269**: 1340–1347.
- Zuo, J., Niu, Q.W., and Chua, N.H.** (2000). Technical advance: An estrogen receptor-based transactivator XVE mediates highly inducible gene expression in transgenic plants. *Plant J.* **24**: 265–273.